

## An Automated Iterative Algorithm for the Quantitative Analysis of *in Vivo* Spectra Based on the Simplex Optimization Method

ROBERT E. LENKINSKI,\* TIM ALLMAN,\* JACOB D. SCHEINER,\*  
AND STANLEY N. DEMING†

\*Department of Radiology, University of Pennsylvania, Philadelphia, Pennsylvania 19104, and

†Department of Chemistry, University of Houston, Houston, Texas 77094

Received June 23, 1988; revised November 7, 1988

The success in utilizing *in vivo* NMR to identify and/or monitor metabolic abnormalities will be determined in large part on the reliability with which the spectral parameters of the metabolites present can be measured. For these reasons it is clear that there is a need for the development of algorithms with which to obtain quantitatively reliable estimates of the spectral parameters of the peaks present. In this report we describe an adaptation of the simplex algorithm which we have found useful in fitting *in vivo* spectral data in the frequency domain. This simplex algorithm was implemented on an IBM-PC AT compatible computer. We evaluated the simplex algorithm on three representative kinds of spectral data: a simulated spectrum,  $^{31}\text{P}$  spectrum of normal calf muscle, and the  $^{31}\text{P}$  spectrum of a pediatric patient with a brain tumor. In each case we generated a set of spectra by adding varying amounts of noise. On the basis of our simulations and the two examples discussed, we conclude that the simplex method generates parameters which are reliable estimates of the areas of the peaks present when the signal-to-noise is above 8:1 for phosphocreatine. We found that the speed of convergence of the algorithm was improved by overestimating the linewidths of the peaks present. We also found that the method converged more rapidly in the presence of a moderate amount of noise. We conclude that the algorithm described here can provide a robust method with which to analyze *in vivo* spectra in a quantitative manner. Because the method requires little user intervention, it lends itself to implementation in a semi-, or fully, automated fashion.

© 1989 Academic Press, Inc.

### INTRODUCTION

The development of spatial localization techniques which generate multinuclear NMR spectra from well-defined volumes of interest (1) has provided the capability of measuring metabolic parameters which can be related to the local disease state. The success in utilizing *in vivo* NMR to identify and/or monitor metabolic abnormalities will be determined in large part by the reliability with which the spectral parameters of the metabolites present can be measured. The statistical validity of the results will depend on both the experimental conditions under which the data were obtained and the method employed for the extraction of the spectral parameters from these data.

There have been several reports in the literature which describe methods for the analysis of *in vivo* spectra. These methods have been reviewed and evaluated recently

by Haselgrove *et al.* (2). These approaches can be divided into time domain analysis (3), maximum entropy methods (4), and frequency domain methods based on spectral analysis carried out after FFT (5). Each of these methods offers its own set of advantages. For example, the time domain analysis methods offer clear advantages in dealing with data that are collected with preacquisition delays. Our own experience with DRESS localization (6) and 3D chemical-shift imaging (7) as well as a review of the literature (8) indicates that truncation artifacts arising from delayed acquisition are present in many of the  $^{31}\text{P}$  spectra obtained by localization methods currently being employed. These artifacts appear as baseline distortions in the frequency domain which can lead to systematic errors in the estimates of areas and linewidths of the peaks present. These methods are computationally intensive, requiring implementation on mainframe level computers or minicomputers rather than microcomputers and, in some cases, requiring user intervention at intermediate stages of analysis. The maximum entropy methods described in the literature suffer from the same disadvantages. For these reasons we explored the possibility of using an algorithm for frequency domain analysis which could be implemented on a microcomputer and required little, or no, user intervention.

We have recently described an algorithm for correcting spectra which contain the truncation artifacts as a result of delayed acquisition in the time domain (9). This method has been implemented as an iterative automated routine. This algorithm involves the use of an iterative estimation of the sum of  $\sin(x)/x$  functions centered

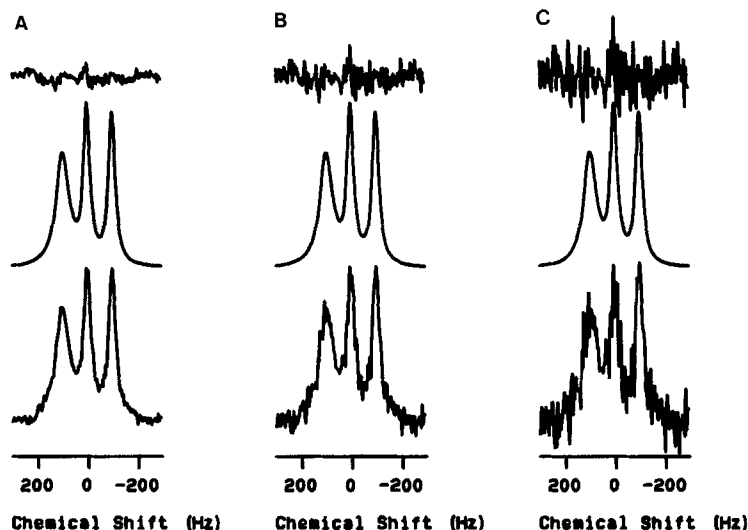


FIG. 1. Three representative simulated spectra (bottom) in the presence of varying amounts of noise, spectra corresponding to the best fit generated by the simplex algorithm (middle), and difference spectra (top). The spectra were simulated for three lines: peak 1,  $\delta = 100$  Hz, linewidth = 60 Hz, and relative area 1.0; peak 2,  $\delta = 0$  Hz, linewidth = 30 Hz, and relative area 1.0; peak 3,  $\delta = -100$  Hz, linewidth = 30 Hz, and relative area 1.0. The signal-to-noise was measured on peak 3 and was 50.9:1 for (A), 20.1 for (B), and 10.2:1 for (C).

at each peak position in the spectrum. The correction is considered complete when the residual baseline distortions are less than the RMS noise (usually four iterations). This baseline correction algorithm has been implemented on an IBM-PC AT compatible computer as part of an overall computer program for the processing of *in vivo* spectral data. In this report we describe an adaptation of the simplex algorithm (vide infra) (10, 11) which we have found useful in fitting *in vivo* data in the frequency domain. This simplex algorithm was also implemented on the IBM-PC AT compatible computer. In the following sections we discuss some of the details of our implementation of this algorithm as well as the potential advantages and disadvantages of this approach.

### EXPERIMENTAL

The simplex algorithm employed was adapted from the variable size simplex program described by Cooper (12). This algorithm was implemented in Turbopascal (Borland) on an AT&T 6300 plus microcomputer equipped with a 80286 CPU and an 80287 math coprocessor (the computer clockspeed is 8 MHz). We modified two parts of the program reported by Cooper (12). These were the initialization subroutine which, in Cooper's version, generates a very elongated and nearly coplanar or colinear initial simplex and the provisions for rejecting the next-worse-vertex which did not work in the published version of the algorithm.

TABLE I  
A Summary of the Results Obtained Using the Simplex Algorithm to Fit Simulated Spectra<sup>a</sup>  
(See Fig. 1 for Examples)

No.	S/N	Iterations	R	Peak 1		Peak 2		Peak 3	
				$\Delta\omega$ (Hz) <sup>b</sup>	Area	$\Delta\omega$ (Hz) <sup>b</sup>	Area	$\Delta\omega$ (Hz) <sup>b</sup>	Area
1	68.6	179	0.07	61	47	30	32	31	32
2	50.9	184	0.06	62	47	31	32	31	33
3	39.4	176	0.07	62	48	31	32	31	32
4	31.9	166	0.09	62	48	31	32	31	32
5	26.7	177	0.10	62	48	31	32	31	33
6	20.1	177	0.13	61	47	31	33	32	33
7	16.1	143	0.16	60	46	32	33	32	33
8	13.5	166	0.19	61	47	32	34	32	33
9	10.2	152	0.25	60	46	33	35	32	33
10	8.2	162	0.31	59	45	34	36	33	34
11	6.0	158	0.42	58	44	36	38	33	35
12	Noise	169	1.00	0.5	-0.3	0.3	0.2	0.4	0.3

<sup>a</sup> The simulations were carried out with the following parameters: peak 1,  $\delta = 100$  Hz, linewidth = 60 Hz, and relative area = 1.5; peak 2,  $\delta = 0$  Hz, linewidth = 30 Hz, and relative area = 1.0; peak 3,  $\delta = -100$  Hz, linewidth = 30 Hz, and relative area = 1.0.

<sup>b</sup>  $\Delta\omega$  is the linewidth at half-height.

The goodness of fit was assessed using a modified crystallographic  $R$  factor (13) defined as

$$R = [\sum (\text{obs} - \text{calc})^2 / \sum (\text{obs})^2]^{1/2}, \quad [1]$$

where obs and calc refer to the experimental and calculated points in the spectrum, respectively. Convergence was considered complete when the  $R$  factor did not change by more than 0.0001.

We evaluated the simplex algorithm on three representative kinds of spectral data. The first set of spectra fitted was a set of simulated spectra containing three lines with linewidths of 60, 30, and 30 Hz and areas in the ratio of 1.5 to 1 to 1, respectively, in the presence of varying amounts of noise. The second set comprised a  $^{31}\text{P}$  spectrum of the calf muscle of a normal volunteer obtained on our General Electric 1.5-T whole-body scanner to which incremental amounts of noise were added. The third set was made up of a DRESS  $^{31}\text{P}$  spectrum of a brain obtained from a pediatric patient with a brain tumor (gemistocytic/desmoplastic astrocytoma). In this spectrum there is probably significant contamination of normal brain tissue.

A set of spectra with different signal-to-noise was obtained by adding varying amounts of white noise to the original spectrum. In all of these cases we fit three parameters per peak: peak position, linewidth, and intensity. Although our implementation of the program permits the specification of any lineshape, we employed

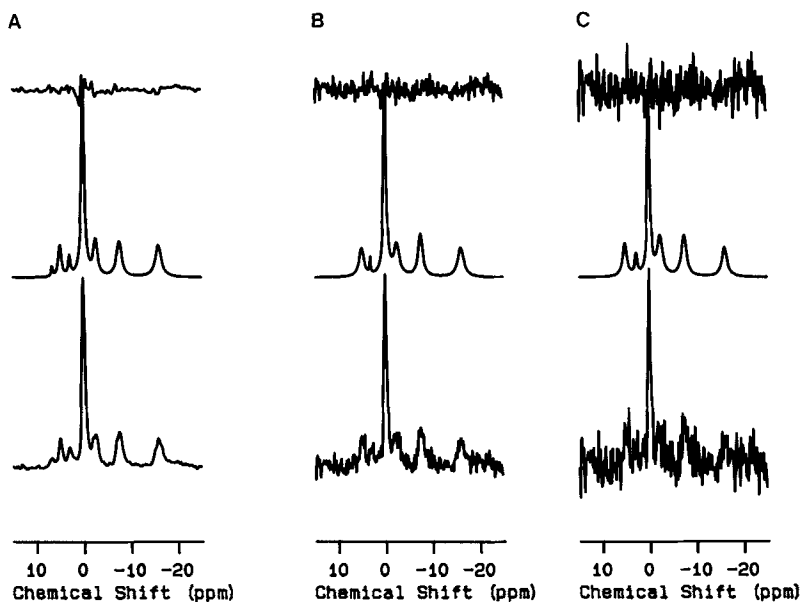


FIG. 2. Three  $^{31}\text{P}$  spectra of calf muscle in the presence of varying amounts of noise (bottom), spectra corresponding to the best fit generated by the simplex algorithm (middle), and difference spectra (top). The signal-to-noise was measured on the PCr peak and was 44:1 for A, 22:1 for B, and 14:1 for C. The experimental spectrum was obtained with a  $90^\circ$  pulse, a 2000-Hz sweep width, 2K data points, and a 4-s repetition delay.

Lorentzian lineshapes in all of the analyses presented here. The signal-to-noise of a given peak was calculated using a standard RMS noise calculation and the peak height of the relevant resonance.

RESULTS AND DISCUSSION

Representative simulated three-line spectra in the presence of varying amounts of noise and the corresponding spectra generated by the simplex algorithm are shown in Fig. 1. The difference between the simulations and the spectra generated by the simplex method are also shown for comparison. In these examples the initial peak positions were obtained using a peak-picking algorithm which was part of the processing software. A summary of the results obtained on the simulated spectra is presented in Table 1. In these fits, we found that the algorithm rarely found a local rather than a global minimum. Although we did not systematically investigate the robustness of the algorithm to the initial values chosen, we did find that the program converged more smoothly when the initial linewidths were overestimated rather than underestimated. The peaks in the experimental spectra have linewidths of between 15 to 40 Hz (this is after multiplication with a 10-Hz exponential filter). Because the experimental spectra are obtained at a digital resolution of about 2 Hz per point, we suggest that choosing a narrow linewidth as an initial estimate may result in computational artifacts associated with the digital resolution. Consequently we started all of our fits with linewidths between 100 and 150 Hz.

The best-fit peak positions generated by the algorithm were all within 2 Hz of the values used as inputs in the simulation. From the results shown in Table 1 it is clear that the maximum difference between the areas and linewidths used in the simulations and the values found by the simplex method was less than 10% even in cases where the signal-to-noise was poor.

We also tested the algorithm by attempting a fit to a spectrum containing pure white noise. The algorithm was started using the same initial estimates as were used in the fits of the simulated three-line spectra described above. The best fit was obtained with the parameters given in the last line of Table 1. In this case the areas

TABLE 2  
A Summary of the Results Obtained from the Fits Generated by the Simplex Algorithm for <sup>31</sup>P Spectra of the Calf Muscle of a Normal Volunteer

Spectrum	S/N (PCR)	S/N (β-ATP)	PCr			β-ATP			Iterations	R
			δ (ppm)	Δω (Hz)	Area	δ (ppm)	Δω (Hz)	Area		
1	44	7.0	0.0	18.5	20.3	-16.1	39.1	7.2	1251	0.12
2	32	4.7	0.0	16.8	19.1	-16.2	40.7	7.0	708	0.24
3	22	3.4	0.0	15.0	16.9	-16.2	33.5	5.8	428	0.33
4	14	2.1	0.0	14.2	15.3	-16.2	30.1	5.2	507	0.48
5	8	1.5	0.0	13.3	14.8	-16.2	26.2	4.0	605	0.54

found by the algorithm were less than 1% of the areas of the original peaks. The algorithm found a small negative peak in this case.

Representative spectra obtained from normal muscle in the presence of varying amounts of noise and the corresponding spectra generated by the simplex algorithm are shown in Fig. 2. The difference between the simulations and the spectra generated by the simplex method are also shown for comparison. The peak-picking routine found seven resonances in the spectra with good signal-to-noise and six resonances

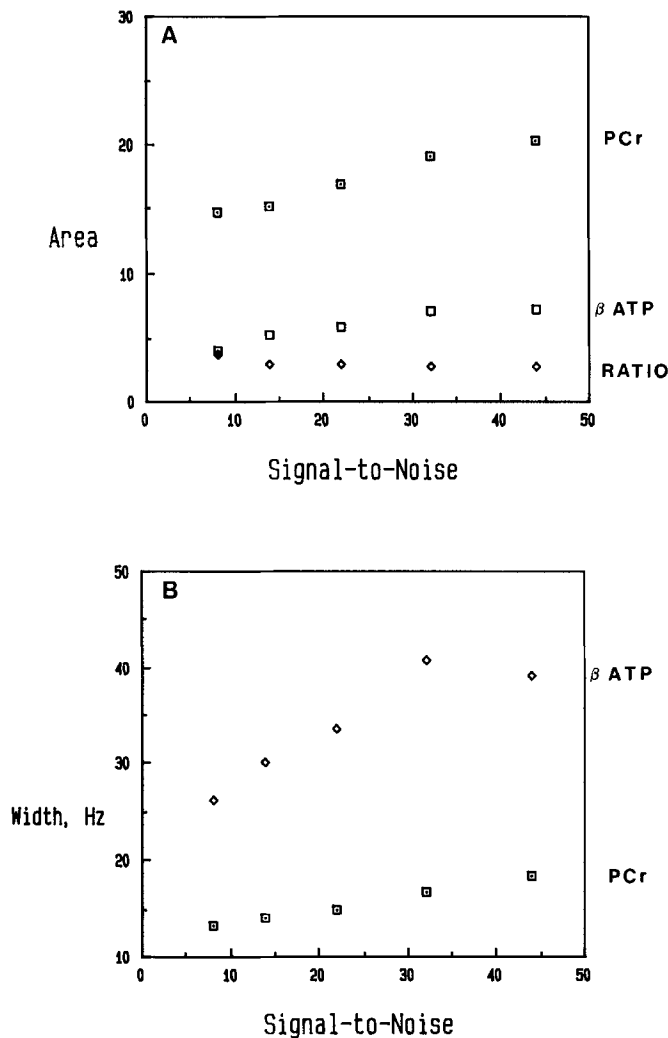


FIG. 3. The variation in the areas (A) and linewidths (B) of the PCr and  $\beta$ -ATP resonances generated by the simplex algorithm from fits to the spectra of normal calf muscle with the signal-to-noise of the spectrum. The results from which these plots were constructed are given in Table 2.

(the program failed to find the peak corresponding to phosphomonoester, PME) in the spectra with intermediate signal-to-noise. As the signal-to-noise became progressively worse, this peak-picking method failed. In these cases we performed the fit by starting with the six peaks found from the spectra with intermediate signal-to-noise. In each of the fits all of the peaks were fit simultaneously; i.e., between 18 and 21 parameters were varied. A partial summary of the results of these fits are compiled in Table 2. The relative values of the areas of the peaks found by the simplex method are similar to the values reported for normal skeletal muscle by Radda and Taylor (14) and by Taylor *et al.* (15).

The simplex converged in between 1251 and 428 iterations at about 1 s per iteration. One of the observations we made in using this program is that the method appears to require fewer iterations to reach a minimum in the presence of intermediate amounts of noise. This is borne out by the results shown in Table 2.

There is a significant variation in both the linewidth and the areas as the signal-to-noise is degraded below 10:1 for phosphocreatine (PCr). The program appears to underestimate both of these parameters in the presence of noise. These trends are

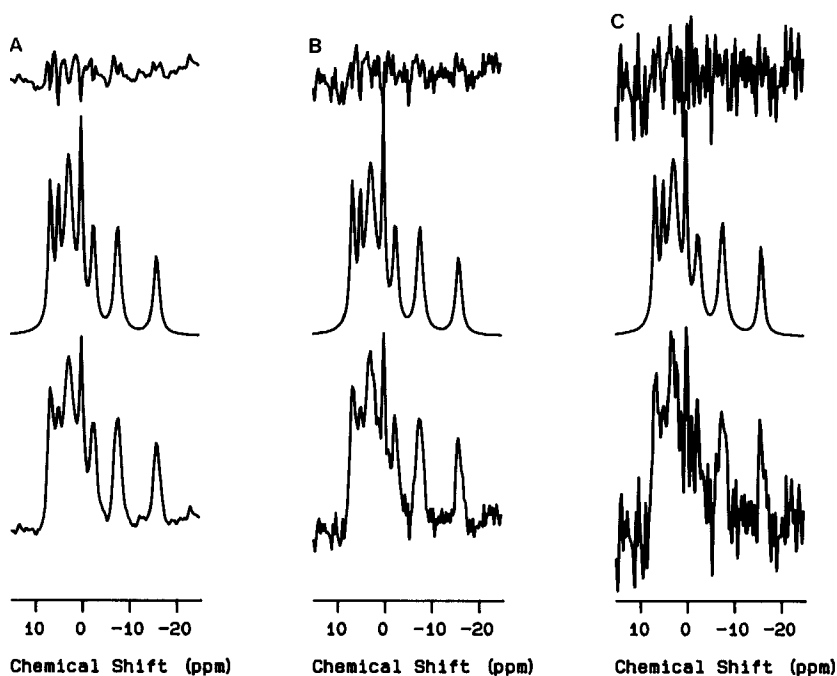


FIG. 4. Three  $^{31}\text{P}$  spectra of the brain of a pediatric patient with a brain tumor in the presence of varying amounts of noise (bottom), spectra corresponding to the best fit generated by the simplex algorithm (middle), and difference spectra (top). The signal-to-noise was measured on the PCr peak and was 19.7:1 for A, 13.5:1 for B, and 8.1:1 for C. The experimental spectrum was obtained from a 3-cm-thick DRESS slice with the same acquisition parameters as described for Fig. 2. The preacquisition delay in this spectrum was 2.1 ms. The baseline distortions present in the spectrum were corrected using the algorithm described in the text.

shown in Fig. 3 in which the values of the linewidths and areas for both PCr and  $\beta$ -ATP are plotted as a function of the signal-to-noise. The results indicate that although the individual areas vary considerably, the ratio of areas of PCr/ $\beta$ -ATP is maintained until the signal-to-noise ratio for  $\beta$ -ATP is worse than 2. It is important to recognize that the worst spectrum analyzed (signal-to-noise of 1.5 on the  $\beta$ -ATP resonance) would be considered unacceptable by most spectroscopists. In this extreme case, the estimates of the areas generated by the simplex algorithm were lower by about 40% for  $\beta$ -ATP and 25% for PCr than those in the original spectrum.

Three representative  $^{31}\text{P}$  spectra obtained from a pediatric patient with a brain tumor in the presence of varying amounts of noise and the corresponding spectra generated by the simplex algorithm are shown in Fig. 4. The difference between the simulations and the spectra generated by the simplex method are also shown for comparison. The peak-picking routine found seven resonances in each of these spectra. In each of the fits performed on this set of spectra all of the peaks were fit simultaneously; i.e., 21 parameters were varied. We found that the peak positions generated by the algorithm did not vary significantly as the noise was increased. A summary of the areas of the various peaks generated by the simplex algorithm is compiled in Table 3. These data are plotted in Fig. 5. There is a relatively large variation in the area found for the inorganic phosphate ( $P_i$ ) peak (4.2 to 11.3) compared to the variations found in the areas of other resonances. We suggest that this large variation is a result of the fact that this resonance has the smallest area and has considerable overlap with both the PME and the phosphodiester (PDE) peaks. It may also reflect the fact that the peak may not have a true Lorentzian lineshape.

There is a significant difference in the values of the areas of many of the peaks found by the simplex algorithm when the signal-to-noise of the spectrum is less than 10:1 for phosphocreatine. In the cases with signal-to-noise above 10:1 the variation is about 10% in the areas for all of the peaks except  $P_i$ .

It is important to note that the simplex algorithm is sensitive to baseline distortions. In all of our fits we assumed that the noise fell randomly about zero; i.e., there was

TABLE 3

A Summary of the Results Obtained Using the Simplex Algorithm to Fit  $^{31}\text{P}$  Spectra of Brain in the Presence of Varying Amounts of Noise

No.	$S/N^a$	Iterations	$R$	Area						
				PME	$P_i$	PDE	PCR	$\gamma$ -ATP	$\alpha$ -ATP	$\beta$ -ATP
1	19.7	1016	0.15	13.3	7.4	37	14.5	11.6	15.0	11.1
2	19.1	1175	0.17	14.0	4.2	43	12.7	11.6	14.9	10.8
3	16.4	925	0.20	13.8	5.7	41	13.2	11.7	15.4	10.8
4	13.5	892	0.25	13.9	5.1	42	12.5	11.8	16.0	10.0
5	11.9	1329	0.29	13.6	7.6	39	13.3	12.3	16.0	9.8
6	8.1	1007	0.38	14.0	6.2	41	12.9	12.9	16.9	10.0
7	5.2	622	0.54	12.9	11.3	37	12.1	12.0	19.5	8.4

<sup>a</sup> The signal-to-noise was measured on the PCR peak.



no systematic baseline roll or DC offset. Although we have not investigated the sensitivity of this algorithm to the magnitude of baseline distortions present, it is clear that the presence of these distortions will result in systematic errors in the fits. As we pointed out earlier we have reported a method for correcting baseline distortions which result from the presence of preacquisition delays in localization methods (8). We have used this method in all of the spectra shown here.

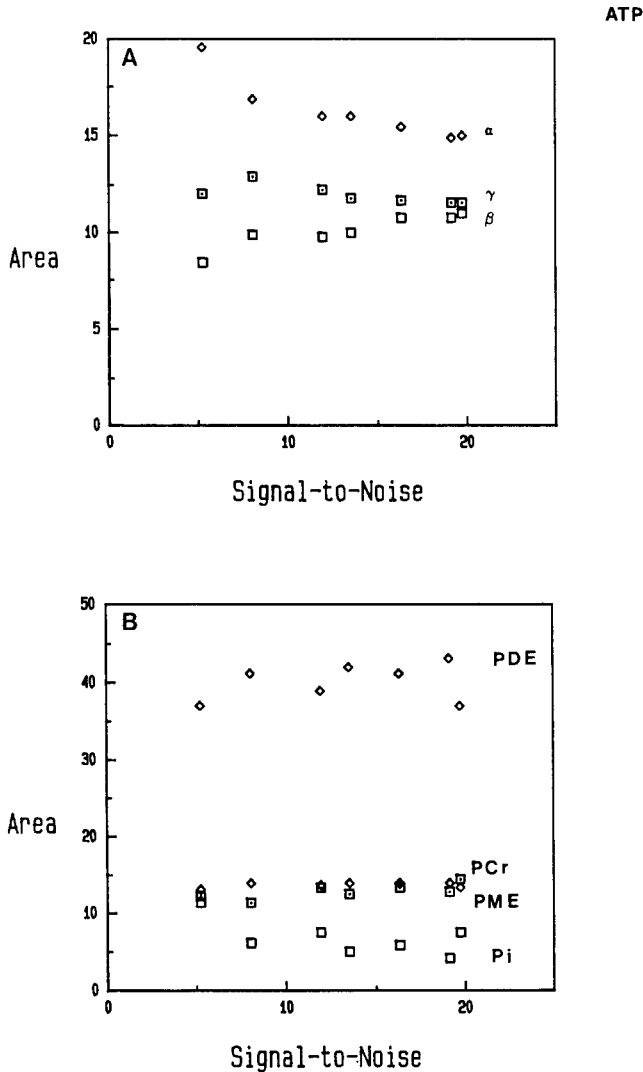


FIG. 5. The variation in the areas of the various resonances generated by the simplex algorithm from fits to the spectra of brain with the signal-to-noise of the spectrum. The results from which these plots were constructed are given in Table 3. For convenience the areas of the ATP resonances are plotted in (A) and the rest are plotted in (B).

## CONCLUSIONS

On the basis of the results presented here we conclude that the simplex method can be employed to fit *in vivo*  $^{31}\text{P}$  spectra. The method requires little operator intervention aside from providing an initial guess for the starting parameters. At present this algorithm requires about 15 min to fit seven peaks in a spectrum made up of 1024 data points. We believe that this time may be reduced substantially by improving the efficiency of the algorithm. We should point out that 15 min is time required to converge from a relatively arbitrarily chosen set of starting parameters. For example, we have made no use of the experimental linewidths or intensities in initiating the simplex. It should be possible to reduce the time required for convergence considerably by providing a better starting point for the algorithm. It should also be possible to fix the resonance frequencies in those cases where the signal-to-noise is poor and fit only the linewidths and intensities. This option could also reduce the time required for convergence. It is also important to note that the method can be employed to fit parts of the spectrum. Each peak can be fit individually or regions of the spectrum can be selected. This option does not exist with many of the time domain analysis methods. On the other hand the simplex method is sensitive to the presence of baseline distortions. This problem may be overcome by phasing and correcting the baseline using the methods we have outlined. However, some of the time domain methods of analysis perform all of these steps in a single fitting algorithm.

On the basis of our simulations and the two examples discussed, we conclude that the simplex method generates parameters which are reliable estimates of the areas of the peaks present when the signal-to-noise is better than 10:1 in brain and 5:1 in muscle. In the case of muscle we found that even though the areas of both the PCr and  $\beta$ -ATP varied individually as the signal-to-noise ratio decreased, the ratio of the areas of these two peaks was relatively constant even at poor signal-to-noise ratios. In both of these cases the peak positions were reliable even at very low signal-to-noise ratios.

In summary we conclude that the algorithm described here can provide a robust method with which to analyze *in vivo* spectra in a quantitative manner. Also, it can be implemented on a relatively inexpensive microcomputer. Because the method requires little user intervention it lends itself to implementation in a semi-, or fully, automated fashion.

## REFERENCES

1. For a review of spatial localization method see W. P. AUE, *Rev. Magn. Reson. Med.* **1**, 21 (1986).
2. J. C. HASLEGROVE, V. H. SUBRAMANIAN, R. CHRISTEN, AND J. S. LEIGH, *Rev. Magn. Reson. Med.* **2**, 167 (1988).
3. See, for example, H. BRAKUIJSEN, R. DE BEER, W. M. M. J. BOVEE, A. M. VAN DE BRINK, A. C. GROGENDIJK, D. VAN ORTMONDT, AND J. W. VAN DER WEEN, in "Signal Processing III: Theory and Applications" (I. T. Young *et al.*, Eds.), p. 1359, Elsevier, Amsterdam, 1986; H. BRAKUIJSEN, R. DE BEER, W. M. M. J. BOVEE, AND D. VAN ORTMONDT, *J. Magn. Reson.* **61**, 465 (1985); M. SHINNAR AND S. M. ELEFF, *J. Magn. Reson.* **76**, 200 (1988).
4. F. NI, G. C. LEVY, AND H. A. SCHERAGA, *J. Magn. Reson.* **66**, 385 (1985); S. SIBISI, *Nature (London)* **301**, 134 (1983).
5. S. J. NELSON AND T. R. BROWN, *J. Magn. Reson.* **74**, 229 (1987).

6. P. A. BOTTOMLEY, T. B. FOSTER, AND R. D. DARROW, *J. Magn. Reson.* **59**, 338 (1984).
7. R. E. LENKINSKI, G. A. HOLLAND, T. ALLMAN, K. VOGELE, H. Y. KRESSEL, R. I. GROSSMAN, H. C. CHARLES, H. R. ENGESETH, D. FLAMIG, AND J. R. MACFALL, *Radiology* **169**, 201 (1988).
8. For examples see D. R. BAILES, D. J. BRYANT, G. M. BYDDER, H. A. CASE, A. G. COLLINS, I. J. COX, P. R. EVANS, R. R. HARMAN, A. S. HALL, S. KHENIA, P. MCARTHUR, A. OLIVER, M. R. ROSE, B. D. ROSS, AND I. R. YOUNG, *J. Magn. Reson.* **74**, 158 (1987); B. D. ROSS, J. T. HELSPER, J. COX, I. R. YOUNG, R. KEMPF, A. MAKEPEACE, AND J. PENNOCK, *Arch. Surg.* **122**, 1464 (1987).
9. T. ALLMAN, G. A. HOLLAND, R. E. LENKINSKI, AND H. C. CHARLES, *Magn. Reson. Med.* **7**, 88 (1988).
10. W. SPENDLEY, G. R. HEXT, AND F. R. HINSWORTH, *Technometrics* **4**, 441 (1962); J. A. NELDER AND R. MEAD, *Comput. J.* **7**, 308 (1965).
11. S. N. DEMING AND S. L. MORGAN, *Anal. Chem.* **45**, 278A (1973); C. L. SHAVERS, M. L. PARSONS, AND S. N. DEMING, *J. Chem. Educ.* **56**, 307 (1976).
12. J. W. COOPER, "Introduction to Pascal for Scientists," p. 186. Wiley, New York, 1981.
13. W. C. HAMILTON, *Acta Crystallogr.* **18**, 502 (1965).
14. G. K. RADDA AND D. J. TAYLOR, *Int. Rev. Exp. Pathol.* **27**, 1 (1985).
15. D. J. TAYLOR, P. J. BORE, D. G. GADIAN, AND G. K. RADDA, *Mol. Biol. Med.* **1**, 77 (1983).